Pharm Res (2015) 32:2863–2876
DOI 10.1007/s11095-015-1669-3

RESEARCH PAPER

A Flow-Cytometry-Based Approach to Facilitate Quantification, Size Estimation and Characterization of Sub-visible Particles in Protein Solutions

Christian Lubich • Mantas Malisauskas • Thomas Prenninger • Thomas Wurz • Peter Matthiessen • Peter L. Turecek • Friedrich Scheiflinger • Birgit M. Reipert

Received: 28 December 2014 / Accepted: 5 March 2015 / Published online: 19 March 2015

ABSTRACT

Purpose Sub-visible particles were shown to facilitate unwanted immunogenicity of protein therapeutics. To understand the root cause of this phenomenon, a comprehensive analysis of these particles is required. We aimed at establishing a flow-cytometry-based technology to analyze the amount, size distribution and nature of sub-visible particles in protein solutions.

Methods We adjusted the settings of a BD FACS Canto II by tuning the forward scatter and the side scatter detectors and by using size calibration beads to facilitate the analysis of particles with sizes below 1 μM. We applied a combination of Bis-ANS (4,4′-dianilino-1,1′-binaphthyl-5,5′-disulfonic acid dipotassium salt) and DCVJ (9-(2,2-dicyanovinyl)julolidine) to identify specific characteristics of sub-visible particles.

Results The FACS technology allows the analysis of particles between 0.75 and 10 μm in size, requiring relatively small sample volumes. Protein containing particles can be distinguished from non-protein particles and cross-β-sheet structures contained in protein particles can be identified.

Conclusions The FACS technology provides robust and reproducible results with respect to number, size distribution and specific characteristics of sub-visible particles between 0.75 and 10 μm in size. Our data for number and size distribution of particles is in good agreement with results obtained with the state-of-the-art technology micro-flow imaging.

KEY WORDS cross-β-sheet structures · flow cytometry · protein aggregates · protein therapeutics · sub-visible particles

Electronic supplementary material The online version of this article (doi:10.1007/s11095-015-1669-3) contains supplementary material, which is available to authorized users.

C. Lubich • M. Malisauskas • T. Prenninger • T. Wurz • P. Matthiessen • P. L. Turecek • F. Scheiflinger • B. M. Reipert (✉)
Baxter Innovation GmbH, Industriestrasse 72, A-1220 Vienna, Austria
e-mail: birgit_reipert@baxter.com

ABBREVIATIONS

Aβ 1–40	Amyloid beta 1–40 peptide
Bis-ANS	4,4′-dianilino-1,1′-binaphthyl-5,5′-disulfonic acid dipotassium salt
DCVJ	9-(2,2-dicyanovinyl)julolidine
DMSO	Dimethyl sulfoxide
D-PBS	Dulbecco's Phosphate-Buffered Saline
preparation Non-Prot	Non-protein particles
preparation Prot	Protein particles without cross-ß-sheet structures
preparation Prot-Crossß	Protein particles containing cross-ß-sheet structures
rFVIII	Recombinant human factor VIII
TEM	Transmission Electron Microscopy
ThT	Thioflavin T
WFI	Water For Injection

INTRODUCTION

Since the introduction of recombinant technologies, an increasing number of protein therapeutics have become available, providing new treatment options for a wide range of diseases (1). Experience with protein therapeutics has shown that many of them bear the risk of inducing unwanted immune responses in patients which can be associated with severe clinical consequences such as a reduction or loss of efficacy, hypersensitivity reactions or neutralization of the natural counterpart. Often, these events are infrequent and only become recognized at a late stage during clinical development or after marketing authorization (2). The most common event is the development of anti-drug antibodies which can diminish

drug efficacy, alter the pharmacokinetic profile of a drug, cause hypersensitivity reactions or cross-react with an endogenous protein. The immunogenic potential of each protein therapeutic is determined by a multiplicity of different factors, which may be patient-, product- or treatment related (3–7). Although research has added considerably to our understanding of the essential determinants of the immunogenicity of protein therapeutics, we are still not able to predict the likelihood of a patient developing unwanted immune responses to a particular protein therapeutic.

Recently, protein missfolding and aggregation were suggested to facilitate the immunogenic potential of protein therapeutics and negatively impact clinical performance (8–10). Missfolding associated with aggregation of endogenous proteins has previously been recognized as a serious problem associated with a number of severe diseases (11). These diseases are characterized by the occurrence of protein aggregates with a highly ordered structure known as cross-spine or cross-β sheet (12). The histology of the resulting insoluble protein aggregate deposits has been called amyloid (11). Maas *et al.* demonstrated that a number of protein therapeutics contain amyloid-like protein aggregates and proposed that these aggregates determine the risk of protein therapeutics inducing unwanted immunogenicity and toxicity (13). This proposal has been supported by findings indicating that amyloid-like protein aggregates can activate the innate immune system, which could be an essential trigger of unwanted immunogenicity (14, 15). However, there is a wide variety of soluble and insoluble protein aggregates, ranging from 1 to 100 nm in size for soluble aggregates and 0.1 to 100 μm for insoluble aggregates (particles) (16). Sub-visible particles are defined as particles between 0.1 and 50 μm in size (17). A more thorough understanding of the potential contribution of the different types of aggregates to the risk of protein therapeutics inducing unwanted immunogenicity is required.

Missfolding and aggregation are intrinsic propensities of proteins when exposed to a number of stress factors which may occur during the manufacturing process of protein therapeutics. Exposure to air-water interface (18), pH changes, light and temperature fluctuations, lyophilization (19), sonication (20), contact with packaging material (21) and sample agitation (22) have been described as potential risk factors for protein missfolding. Moreover, non-protein particles present in protein therapeutics may provide nucleation sites and facilitate protein aggregation (23–27). In addition, protein interaction with silicone oil, which is widely used to prevent protein fouling on surfaces and as lubricant, may promote protein aggregation (28, 29). Therefore, manufacturers of protein therapeutics are expected to develop protein formulations that adequately minimize the impact of the various stress factors on the native protein structure (8, 30). For this purpose, suitable analytical tools are required to closely monitor and characterize protein aggregates and non-protein particles. Currently available analytical technologies such as nanoparticle tracking analyses, flow microscopy, electrophoretic light scattering, light obscuration, electrospray differential mobility analyses and resonant mass measurement have provided important information. However, these technologies cannot simultaneously characterize the composition, structure, chemistry, amount and size of protein aggregates in a single sample. Thus, there is a need for additional analytical tools which facilitate both the detection of a wide size range of protein aggregates and an assessment of their composition and structural properties. More than two decades ago, flow cytometry was already used to analyze amyloid plaques (31), but it was only recently that Mach *et al.* (32) and Ludwig *et al.* (33) introduced flow cytometry as a suitable analytical tool to characterize sub-visible particles. They provided evidence that flow cytometry might be a promising technology for efficient monitoring of sub-visible particles in therapeutic protein formulations. Here, we describe a flow-cytometry-based approach which facilitates the simultaneous analysis of amount, size distribution and nature of sub-visible particles in protein solutions. We paid particular attention to the analysis of potential cross-β-sheet structures because they were suggested to determine the risk of protein therapeutics inducing unwanted immunogenicity and toxicity (13). Furthermore, we present data demonstrating the applicability of flow cytometry to assess the interaction of proteins with silicone oil droplets without the need for labeling the interaction partners.

MATERIALS & METHODS

Sample Preparation for Analysis of Sub-visible Particles

Non-Protein Particles: Silicone Oil Droplets (Preparation Non-Prot)

Silicone oil droplets were prepared as described by Mach *et al.* (32). In brief, 10 ml Dulbecco's PBS (D-PBS; Invitrogen Corporation) were filled into a 30 ml BD Syringe Plastipak (BD Bioscience) which contains special silicone lubrication to facilitate smooth plunger moves. Silicone oil particles were produced by vertically shaking the filled syringe manually for 2 min.

Protein Particles Without Cross-ß-Sheet Structures: A Complex Consisting of Biotinylated Bovine Serum Albumin and Avidin (Preparation Prot)

Biotinylated bovine serum albumin (Biotin-BSA) and avidin from egg white (both Sigma-Aldrich) were mixed together at concentrations of 50 μg/ml Biotin-BSA and 12 μg/ml avidin. The mixture was incubated at room temperature for 60 min. The resulting Biotin-BSA-avidin complex was diluted 1:10

with D-PBS and stored at ≤−60°C prior to analysis. The absence of cross-β-sheet structures was confirmed using a thioflavin T assay as described below in the section "Thioflavin T (ThT) assay" (Fig. 1a). If not otherwise indicated, the final working concentration of preparation Prot was 5.4 μg/ml.

Protein Particles Containing Cross-ß-Sheet Structures: Aggregated Amyloid Beta 1–40 Peptide (Preparation Prot-Crossß)

One milligram amyloid beta 1–40 peptide (Aβ 1–40; Bachem AG) was dissolved in 115 μl water for injection (WFI; Pharma Hameln) to obtain a final concentration of 2 mM. This solution was incubated at 2–8°C for 168 h. The resulting material was diluted with WFI to a final concentration of 15 μg/ml, aliquoted and stored at ≤−60°C prior to analysis. The presence of cross-β-sheet structures was confirmed using a ThT assay and transmission electron microscopy as described below in the sections "Thioflavin T (ThT) assay" and "Transmission electron microscopy" (Fig. 1a, b). If not otherwise indicated, the final working concentration of preparation Prot-Crossß was 13.1 μg/ml.

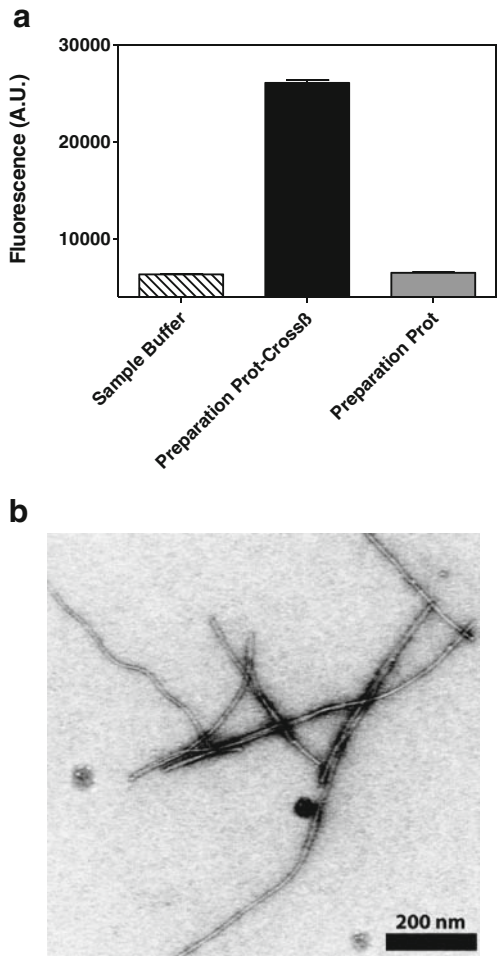

Fig. 1 Confirmation of cross-β-sheet structures by ThT assay and electron microscopy (**a**) Protein samples "Preparation Prot-Crossß" and "Preparation Prot" were mixed with ThT as described in the section Materials and Methods and subsequently analyzed for fluorescence using a Synergy™ 4 Hybrid Microplate Reader. "Sample Buffer" was included as negative control. Three replicates were analyzed for each sample. Results are presented as mean + standard deviation. The high fluorescence signal for sample "Preparation Prot-Crossß" indicates the presence of cross-β-sheet structures. (**b**) The morphology of cross-β-sheet containing protein aggregates in sample "Preparation Prot-Crossß" analyzed by transmission electron microscopy as described in the section Materials and Methods.

Thioflavin T (ThT) Assay

ThT binding assays were done as described (34). A stock solution of ThT (Sigma-Aldrich) was prepared at a concentration of 1 mM in D-PBS and stored at 4°C, protected from light. For ThT fluorescence measurements, protein samples were diluted with D-PBS to a final protein concentration of 10 μg/ml and mixed with the ThT stock solution to a final concentration of 20 μM. Three replicates were analyzed for each sample. The ThT fluorescence measurements were done on a Synergy™ 4 Hybrid Microplate Reader (BioTeK) using clear bottom, black, special optic plates (Corning Life Sciences). The signals were recorded from the bottom of a microtiter plate, with the excitation set at 440±9 nm and the emission set at 485±9 nm.

Transmission Electron Microscopy (TEM)

TEM micrographs were collected using a JEM-120B microscope (JEOL) operating with an accelerating voltage of 80 kV. Typical nominal magnifications ranged from 40,000 to 80,000 X. Samples were deposited on formvar-coated 400-mesh copper grids and negatively stained with 1% aqueous uranyl acetate (Sigma-Aldrich).

Human Recombinant Factor VIII

The human recombinant factor VIII (rFVIII) was production intermediate obtained from Baxter BioScience. It was dialyzed against D-PBS containing calcium- and magnesium chloride (Invitrogen Corporation) and stored at ≤−60°C prior to analysis.

Comparison of MFI and FACS Technologies

Solutions of rFVIII (20 μg/ml) containing increasing amounts of spiked silicone oil droplets were used.

Interaction Studies of Silicone Oil Droplets and Protein

A solution of rFVIII (73.4 μg/ml) in D-PBS was filtered through a 0.22 μm pore filter (Merck Millipore) and subsequently mixed with D-PBS enriched with silicone oil droplets. The mixture was prepared 10 min prior to analysis. The

rFVIII concentration in the final solution was 20 µg/ml. Control samples were prepared by diluting the filtered rFVIII solution and by diluting the D-PBS enriched with silicone oil droplets with equal volumes of D-PBS.

Detection, Size Estimation, Characterization and Quantification of Sub-visible Particles by Flow-Cytometry

All samples were analyzed using a 3-laser (405, 488 and 630 nm) 8-color BD FACS Canto II flow cytometer (BD Bioscience) which was calibrated on a weekly basis using CS&T beads (BD Bioscience). A low and constant background signal, essential for reproducibility and stable performance of the analysis, was achieved by appropriate cleaning and equipment preparation using BD FACS Clean and Rinse solutions (BD Bioscience). The flow rate of the cytometer was set to the lowest level (~10 µl/min) while acquiring and recording each sample for 300 s.

Settings of the BD FACS Canto II Flow Cytometer

Thresholds on FSC and SSC were set to 250; PMT Voltages: 405 V for FSC and 210 V for SSC; PMT 530/30 (blue laser 488 nm): 360 V; PMT 450/50 (violet laser 405 nm): 380 V; Window Extension: 7

Detection and Size Estimation of Sub-visible Particles

To verify the resolution capability of 0.75 µm particles, voltages for forward scatter (FSC) and side scatter (SSC) as well as the threshold levels for these channels were adjusted using Fluoresbrite® YG Carboxylate Size Range beads (Polyscience Inc.). The size of sub-visible particle was estimated by setting different size ranges using beads with defined diameters of 0.75, 1, 2, 4.5, 6 and 10 µm. In most experiments, size ranges were set between the peak maxima of each bead population in a FSC histogram.

When the flow-cytometry-based technology was compared with micro-flow imaging, the size ranges for the flow-cytometry approach were set from each peak maxima up to the right end of the scale. Size ranges were adjusted for each experiment.

Characterizing the Nature of Sub-visible Particles

To distinguish protein from non-protein sub-visible particles, samples were stained with the fluorescent dye 4,4′-dianilino-1, 1′-binaphthyl-5,5′-disulfonic acid dipotassium salt (Bis-ANS; Sigma-Aldrich) which binds to hydrophobic patches contained in proteins (35). Bis-ANS was excited with the violet laser (405 nm). The emitted fluorescence which has a peak maximum at 515 nm, was detected with a 450/50 band-pass filter in the violet detector array.

Protein sub-visible particles were further characterized using Bis-ANS in combination with the fluorescence dye 9-(2,2-Dicyanovinyl)julolidine (DCVJ; Sigma-Aldrich) which binds to cross-β-sheet structures present in aggregated proteins (35–37). DCVJ was excited with the violet laser (405 nm) and the blue laser (488 nm). The emitted fluorescence which has a peak maximum at 480–505 nm (35), was detected with a 530/30 band-pass filter in the blue octagon detector array.

Bis-ANS was dissolved in WFI to a final concentration of 1 mM. DCVJ was dissolved in 73% DMSO/WFI to a final concentration of 4 mM. Both dye stock solutions were covered with aluminum foil and stored in the dark at +4–8°C. They were stable for at least 3 months.

Quantification of Sub-visible Particles

CountBright™ Absolute Counting Beads (Invitrogen Corporation) were used to quantify particles. The bead solution was prepared according to the manufacturer's instructions and added together with Bis-ANS (final concentration 20 µM) and DCVJ (final concentration 25 µM) to each sample prior to analysis.

Data Analysis

Data for each sample was stored as an FCS 3.0 file and subsequently analyzed by FlowJo 10.0.6. (Tree Star Inc.) using the following gating strategy [see Supplement Figure 1 for further details]: CountBright™ Absolute Counting Beads were gated using the 660/20 band-pass filter in the red detector array. Gating on protein sub-visible particles was done in the Bis-ANS channel (violet detector array, 450/50 band-pass filter) by acquiring a non-protein sub-visible particle control (preparation Non-Prot) as a negative control reference. Protein sub-visible particles bearing a cross-β-sheet structure were acquired in the DCVJ channel (blue detector array, 530/30 band-pass filter) using preparation Prot as a negative reference control and preparation Prot-Crossß as a positive control for cross-β-sheet structures.

Each sample was analyzed in 3 replicates. The average concentrations of sub-visible particles for total sub-visible particles, non-protein sub-visible particles, protein containing sub-visible particles and cross-ß-sheet containing protein sub-visible particles were calculated taking the dilution factors of the dyes and the CountBright™ Absolute Counting Beads into account. If not otherwise indicated, the average concentration of sub-visible particles refers to particles between 0.75 and 10 µm in size.

Single Particle Detection *Versus* Swarm Detection

To verify that the flow-cytometry based technology detects single particles rather than swarms of multiple particles, we serially diluted preparation Prot-Crossß and analyzed total particles, protein particles and cross-β-sheet-containing protein particles for each dilution step. We compared the total particle concentrations obtained for each dilution step taking the dilution factor into account.

Validation of the Flow-Cytometry-Based Technology

We evaluated the reliability and accuracy of the flow-cytometry-based technology by assessing multiple properties as suggested for this purpose by current regulatory guidelines for bioanalytical method validation (38, 39). Assessed properties included potential carry-over effects of the dye or the protein, specificity, precision, accuracy, dilution linearity and relative sensitivity.

Except for carry-over effects and relative sensitivity, the samples for validation of the technology were prepared as described above in the section "Detection, size estimation, characterization and quantification of sub-visible particles by flow-cytometry".

Assessing Potential Carry-Over Effects of Protein Particles and Fluorescence Dyes

To assess potential carry-over effects of protein particles and dyes, we analyzed preparation Prot-crossß with and without washing the tubing system after analysis of each of three replicates and compared the average concentrations of sub-visible particles for total sub-visible particles, non-protein sub-visible particles, protein containing sub-visible particles and cross-ß-sheet containing protein sub-visible particles. To assess carry-over effects of the dyes, we analyzed an unstained Prot-crossß sample directly after the three replicates of the stained Prot-crossß sample. The unstained Prot-crossß sample was not stained with Bis-ANS or DCVJ, therefore, any fluorescence staining would reflect a carry-over effect of the dyes which are still present in the tubing system.

Assessing Specificity

The specificity of the technology was verified using positive and negative controls for the dyes (preparations Non-Prot, Prot, Prot-Crossß).

Assessing Precision

The precision of the technology was defined as inter- and intra-assay variation. We analyzed preparation Prot-Crossß in 6 independent experiments for inter-assay variation and in 6 experiments run in parallel for intra-assay variation. The coefficients of variation (CV %) for inter- and intra-assay were calculated individually for total particles, for protein particles and for cross-β-sheet-containing protein particles.

Assessing Accuracy

The accuracy of the method (in CV %) was calculated as variability in the number of total sub-visible particles detected for the different size ranges. For this purpose, the same sample was analyzed 6 times on the same day.

Assessing Dilution Linearity

The linearity of the technology was assessed as described in the section "Single particle detection versus swarm detection".

Assessing the Relative Sensitivity

The relative sensitivity of the method was calculated as the minimum concentration of particles which could be analyzed with a maximum CV of 25%. For this purpose, beads of the Fluoresbrite® YG Carboxylate Size Range Kit I & II were serially diluted with D-PBS. These beads were not stained with Bis-ANS or DCVJ but emitted light in the respective fluorescence PMTs. Each dilution was analyzed ten times and CVs% were calculated for each dilution step for the PMTs detecting total sub-visible particles, non-protein sub-visible particles, protein containing sub-visible particles and cross-ß-sheet containing protein sub-visible particles.

Micro-Flow Imaging

Micro-flow imaging (MFI) was done using a DPA4200 Flow Microscope (Brightwell Technologies). The pump speed was set to 0.17 ml/min during sample measurement. The flow cell was flushed with water before each analysis. Optimized illumination of the background was done using product filtered through 0.22 µm pores. Baseline runs with WFI to verify and quantify system cleanliness were done before the first and after the last sample was measured. 800 µl of a sample was needed for each sample run with an analyzed volume of approximately 450 µl. During each sample run, images were stored for evaluation of particles and for use of the electronic filter settings afterwards. After analyses, particle concentrations were categorized according to the particle sizes ≥1, ≥2, ≥5, ≥10, ≥25, ≥50 and ≥70 µm.

To compare state-of-the-art MIF technology and our flow cytometry approach, we analyzed samples of rFVIII with or without silicone oil droplets using both technologies. rFVIII was freshly reconstituted before measurement. The silicone oil droplets were generated as previously described, diluted to two concentrations (non-Protα; non-Protβ) and mixed with

rFVIII prior to analysis. We compared the concentration of total sub-visible particles of different size ranges. For this purpose, the size ranges of the flow-cytometry-based technology were adapted to those covered by MFI, namely ≥ 1, ≥ 2, ≥ 5 and ≥ 10 μm. rFVIII without non-protein silicone particles was included as a control. Samples to be analyzed by flow-cytometry were prepared as described in section "Detection, size estimation, characterization and quantification of sub-visible particles by flow-cytometry".

Statistical Analysis

The CV % expresses the assay variation as a percentage of the mean and was calculated as follows: (standard deviation/mean)*100

The standard deviation was calculated using

$$\sqrt{\frac{\sum (x-\bar{x})^2}{(n-1)}}$$

where x is the sample mean (number1, number2,…) and n is the sample size.

RESULTS

Detection, Size Estimation and Quantification of Sub-visible Particles Using Flow-Cytometry

The BD FACS Canto II flow cytometer is usually set up to analyze cells between 5 and 20 μm in size. We adjusted the settings of the BD FACS Canto II to facilitate the analysis of sub-visible particles with sizes below 1 μm. We achieved the best signal to noise ratio by setting the thresholds of FSC and SSC to 250 and by setting the voltages of these detectors to 405 V for FSC and 210 V for SSC. When we compared Height and Area for the recording of FSC and SSC signals, we did not see any difference in outcome which is why we used Area for the rest of the studies. A representative example for the appearance of sub-visible particles using these settings is shown in Fig. 2a which reflects the analysis of a preparation of aggregated Aß1-40 peptide (preparation Prot-Crossß). When we used the same settings for the analysis of size calibration beads, we could establish a reproducible working size range of 0.75 to 10 μm which is reflected in Fig. 2b. The average

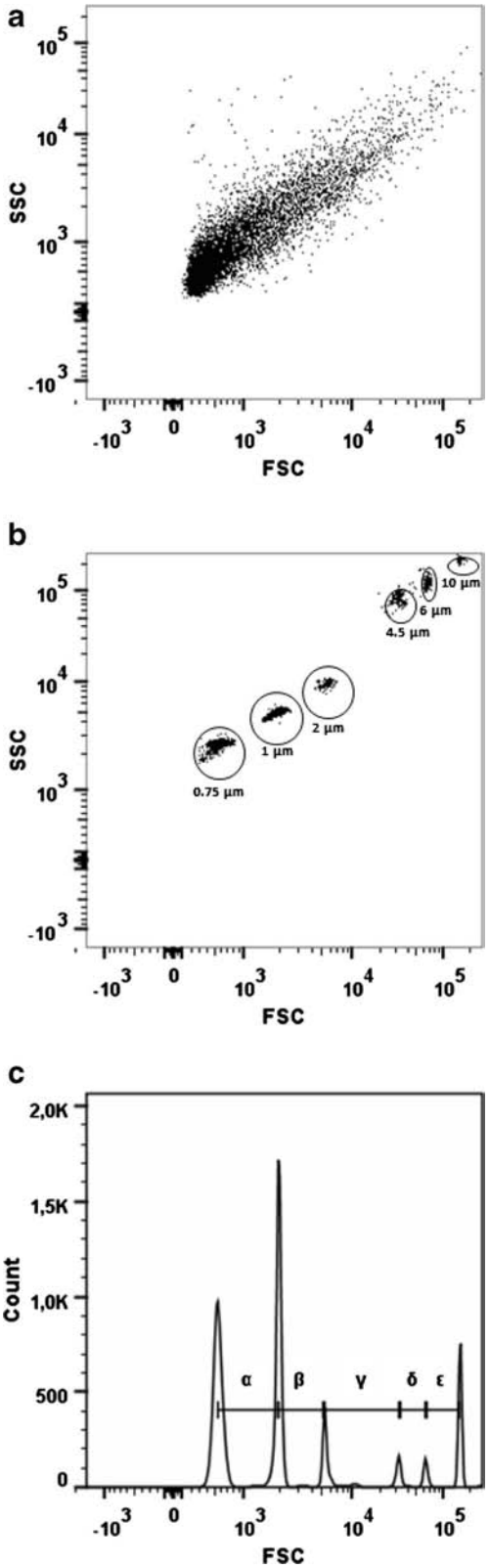

Fig. 2 Detection and size distribution of sub-visible particles. (**a**) Presented is a representative example for a dot plot of Forward Scatter (FSC) *versus* Side Scatter (SSC) using logarythmic scales. A sample of aggregated Aß1-40 peptide was generated and analyzed as described in the section Materials and Methods. (**b**) A representative example is shown for the calibration of the BD FACS Canto II using a mixture of size calibration beads with sizes of 0.75, 1, 2, 4.5, 6 and 10 μm. (**c**) Establishment of specific size ranges using the peak maxima for each size as determined by the size calibration beads in the FSC channel: 0.75-1 μm (α), 1–2 μm (β), 2–4.5 μm (γ), 4.5–6 μm (δ) and 6–10 μm (ε).

concentrations of sub-visible particles refer to particles between 0.75 and 10 μm in size.

Next, we established more specific size ranges using the peak maxima for each size as determined by the size calibration beads in the FSC channel, e.g. 0.75–1, 1–2, 2–4.5, 4.5–6 and 6–10 μm (Fig. 2c). When we applied these specific size ranges to the analysis of preparation Prot-Crossß, we obtained the following results for the size distribution of sub-visible particles in this preparation: 789,374 particles/ml with sizes between 0.75 and 1 μm; 246,767 particles/ml with sizes between 1 and 2 μm; 163,747 particles/ml with sizes between 2 and 4.5 μm; 20,970 particles/ml with sizes between 4.5 and 6 μm and 10,284 particles/ml with sizes between 6 and 10 μm.

Characterization of Sub-visible Particles

After establishing specific size ranges, we were interested to differentiate particles containing protein from non-protein particles and to identify cross-β-sheet structures in protein containing particles. We tested different combinations of fluorescent dyes which bind to specific structures in proteins to find the optimum combination with respect to minimal spectral overlap, absence of dye-induced artifacts and reproducibility of staining behavior. We selected an optimized combination of Bis-ANS and DCVJ. Bis-ANS binds to hydrophobic patches on protein surfaces resulting in about 100-fold increase in its fluorescence intensity (35). The results presented in Fig. 3a–c reflect representative examples using Bis-ANS as a protein stain. Presented are the analyses of silicone oil particles (preparation Non-Prot, Fig. 3a), of a complex containing biotinylated BSA and avidin (preparation Prot, Fig. 3b) and of aggregated Aß1-40 peptide (preparation Prot-Crossß, Fig. 3c). While the protein-containing samples (preparations Prot and Prot-Crossß) showed binding to Bis-ANS associated with an increase in the fluorescence signal (Fig. 3b and c), staining of silicone oil droplets (preparation Non-Prot) with Bis-ANS did not cause an increase in the fluorescent signal (Fig. 3a). In addition to silicone oil particles, we tested other non-protein particles such as glass beads, polystyrene beads and latex beads, which generated negative results similar to those obtained with silicone oil particles.

DCVJ binds to cross-β-sheet structures in aggregated proteins (35–37). Data presented in Fig. 3e–g reflect representative examples using DCVJ staining. Whereas preparation Prot-Crossß (Fig. 3g) contained cross-ß sheets, preparations Non-Prot (Fig. 3e) and Prot (Fig. 3f) did not contain cross-ß sheets. The Prot-Crossß preparation bound DCVJ which was associated with an increase in the fluorescence signal (Fig. 3g). The preparations Non-Prot and Prot did not bind DCVJ (Fig. 3e and f).

After establishing the suitability of Bis-ANS staining for the differentiation of protein particles from non-protein particles and the suitability of DCVJ staining for the staining of cross-ß sheets in protein particles, we tested the combination of both dyes. The results of these studies are shown in Fig. 3d and h, presenting overlays of preparations Non-Prot, Prot and Prot-Crossß. The results illustrate that the combination of Bis-ANS and DCVJ is suitable to facilitate the differentiation of protein particles from non-protein particles and the identification of protein particles that contain cross-ß sheets.

Single Particle Detection Versus Swarm Detection

Using flow-cytometry, the analysis of individual particles with a size below 1 μm can be challenging because it involves the measurement of dim signals which are close to the detection limit of the instrument. Recently, the phenomenon of swarm detection was reported which describes the detection of several small particles at the same time resulting in an underestimation of the absolute number of particles (40, 41). To verify the capacity of the FACS technology to detect single particles, we serially diluted a solution of aggregated Amyloid beta 1–40 peptide (preparation Prot-Crossß) and quantified the numbers of total particles, protein containing particles without cross-β-sheet structures and protein containing particles with cross-β-sheet structures for each dilution step. Results presented in Fig. 4 confirm the linearity of the FACS technology and indicate a linear relationship between the protein concentration of the analyte and the detected particle count for each of the particle types analyzed. Moreover, the total concentrations of particles were independent of the dilution factor. When considering the total concentration of particles (0.75–10 μm) calculated for each of the six dilution steps, we calculated a mean of 2,235,748 particles /ml with a CV of 10.71% for total particles; a mean of 2,142,220/ml with a CV of 14.95% for protein particles without cross- β-sheets and a mean of 2,048,453 with a CV of 18.21% for cross-β-sheet-containing protein particles. These results indicate that the number of counted particles is independent of the dilution factor which supports the detection of single particles rather than swarms of small particles.

Validation of the Flow-Cytometry-Based Technology

To verify reproducibility and accuracy of the FACS technology we validated it by assessing parameters suggested by current regulatory guidelines for bioanalytical method validation (38, 39).

Carry-over effects for both the dye and the protein particles were observed when two samples were analyzed without a washing step of the tubing system in between. Therefore, we included a washing step after each sample acquisition using BD FACS Rinse for 60 s at the highest flow rate.

The specificity of the technology was validated by assessing a range of control preparations: preparation Non-Prot

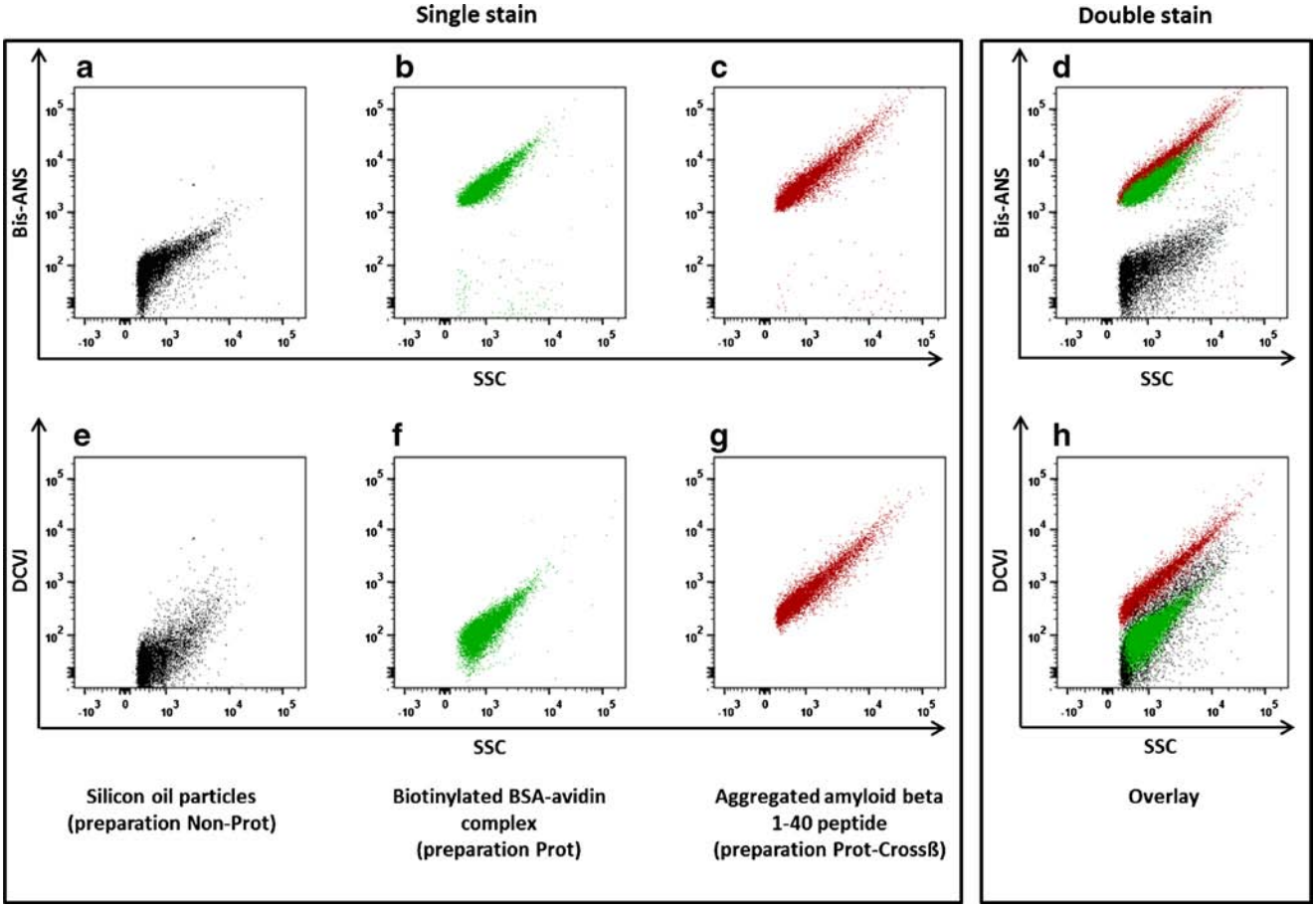

Fig. 3 Characterizing the nature of sub-visible particles by staining with Bis-ANS and DCVJ. (**a**–**c**) Comparison of silicone oil particles (preparation Non-Prot) with a complex of Biotinylated BSA and avidin (preparation Prot) and with a preparation of Aggregated amyloid beta 1–40 peptide (preparation Prot-Crossß) for their binding to Bis-ANS, a fluorescent dye which specifically binds to hydrophobic patches in proteins. Binding of Bis-ANS to the preparations of protein particles "Preparation Prot" and "Preparation Prot-Crossß" resulted in an increased Bis-ANS fluorescence intensity. In contrast, "Prepartion Non-Prot" containing silicone oil particles did not bind to Bis-ANS. (**e**–**g**) Comparison of silicone oil particles (preparation Non-Prot) with a complex of Biotinylated BSA and avidin (preparation Prot) and with a preparation of Aggregated amyloid beta 1–40 peptide (preparation Prot-Crossß) for their binding to DCVJ, a fluorescent dye which specifically binds to cross-β-sheets contained in protein particles. Binding of DCVJ to "Preparation Prot-Crossß" resulted in an increased DCVJ fluorescence intensity. In contrast, "Preparation Non-Prot" containing silicone oil particles and "Preparation Prot" containing protein particles without cross-β-sheets did not bind to DCVJ. (**d**, **h**) Double-staining of silicone oil particles (preparation Non-Prot), a complex of Biotinylated BSA and avidin (preparation Prot) and a preparation of Aggregated amyloid beta 1–40 peptide (preparation Prot-Crossß) with Bis-ANS and DCVJ. Presented are an overlay of fluorescence in the Bis-ANS channel (**d**) and an overlay of fluorescence in the DCVJ channel (**h**) for all three preparations.

containing silicone oil particles, preparation Prot containing protein particles without cross-ß sheets and preparation Prot-Crossß containing protein particles with cross-ß sheets. Our validation data indicate that Bis-ANS binds to protein particles (preparations Prot and Prot-Crossß) but not to non-protein particles (preparation Non-Prot). Moreover, Bis-ANS does not bind to glass beads, polystyrene beads or latex beads. DCVJ only binds to preparation Prot-Crossß containing protein particles with cross-β sheets, but not to preparations Non-Prot or Prot (Fig. 3 and Supplement Figure 1).

The precision of the technology was validated as inter- and intra-assay variation. We analyzed preparation Prot-Crossß containing protein particles with cross-ß sheets in 6 independent experiments for inter-assay variation and in 6 parallel experimental runs for intra-assay variation. The coefficient for inter- and the intra-assay variation (CV %) was calculated for total particles, for protein-containing particles and for cross-β-sheet-containing protein particles. The CVs for inter-assay variation were 10.32% for total particles, 10.36% for Bis-ANS positive protein particles and 16.32% for DCVJ positive cross-ß-sheet-containing particles (Supplement Table 1A). The CVs for intra-assay variation were 3.92% for total particles, 3.79% for Bis-ANS positive protein particles and 2.05% for DCVJ positive cross-ß-sheet-containing particles (Supplement Table 1B).

The accuracy of the method (in CV %) was calculated as the variability in the number of total particles detected in 1 ml for the different pre-defined size ranges. For this purpose, the same sample was analyzed 6 times on the same day. The CVs in the respective size ranges were 13.87% for the size range 0.75–1 µm; 15.18% for the size range 1–2 µm; 19.67% for the size range 2–4.5 µm; 20.13%

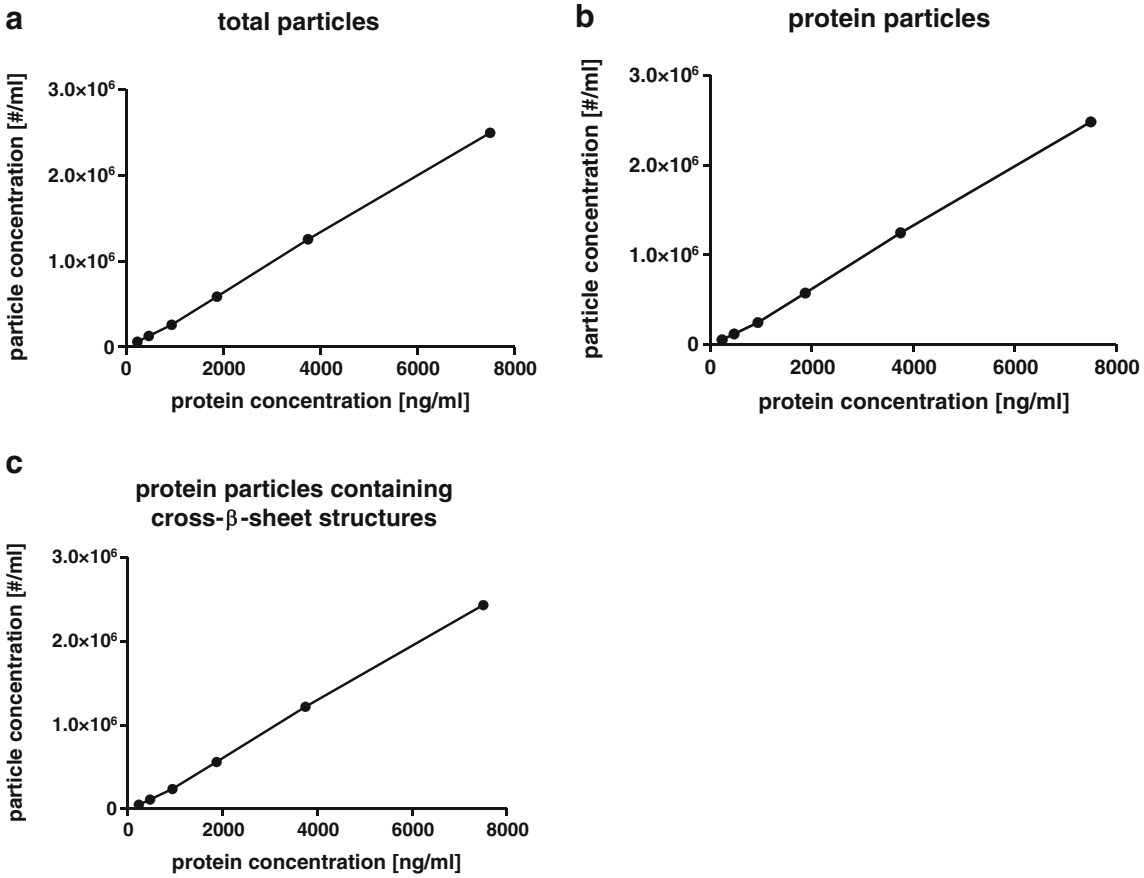

Fig. 4 Linear relationship between protein concentration and detected particle count in the analysis of a preparation of protein particles using flow-cytometry. A preparation of aggregated Aß1-40 peptide (preparation Prot-Crossß), generated as described in the section Materials and Methods, was serially diluted. Each dilution was stained with Bis-ANS and DCVJ and subsequently analyzed by flow cytometry for the concentration of total particles (**a**), protein particles (**b**) and cross-β-sheet containing particles (**c**). Presented are protein concentration and the concentration of sub-visible particles in the size range of 0.75–10 μm. Each dilution was analyzed in 3 replicates for the concentration of sub-visible particles, mean numbers are presented.

for the size range 4.5–6 μm and 20.56% for the size range 6–10 μm (Supplement Table 1C).

Based on the validation results, we conclude that all CVs% for intra- and inter-assay variation as well as for accuracy met the pre-defined acceptance criteria which were set to a maximum of 25%, which is in compliance with current regulatory guidelines (38, 39).

The linearity of the technology was assessed by serially diluting preparation Prot-Crossß and analyzing total particles, protein particles and cross-β-sheet-containing protein particles for each dilution step. Our results as presented in Fig. 4 indicate a direct relation between the concentration of the analyte and the particle count for each type of particle tested.

The relative sensitivity of the technology was defined as the minimum number of particles in 1 ml which can be reproducibly detected by the flow cytometer when a maximum CV of 25% is accepted. We serially diluted beads from the Fluoresbrite® YG Carboxylate Size Range Kit I & II, measured each dilution step 10 times and calculated the CV% for each dilution step. The lowest bead concentration which could be analyzed with a maximum CV of 25% was 1500 beads per ml.

In summary, the validation results confirm that the flow-cytometry based technology for the analysis of sub-visible particles with a size range 0.75–10 μm meets all requirements for bioanalytical methods as suggested by current regulatory guidelines (38, 39).

Comparative Analysis of Sub-visible Particles Using Flow-Cytometry and State-of-the-Art Micro-Flow Imaging

Next, we were interested to know how results obtained with the flow-cytometry-based technology compare to results obtained with the state-of-the-art technology micro-flow imaging. We used a preparation of rFVIII mixed with two different non-protein silicone particle preparations (preparation Non-Protα and Non-Protβ, Fig. 5a and b) and analyzed the concentration of total sub-visible particles in different size ranges. For this purpose, the size ranges of the flow-cytometry-based technology were adapted to the size ranges covered by the micro-flow imaging technology, namely ≥1, ≥2, ≥5 and ≥10 μm. The results obtained with the micro-flow imaging

technology (Fig. 5a) were in good agreement with those obtained with the flow-cytometry-based technology (Fig. 5b). Both technologies showed a concentration-dependent increase in sub-visible particle count after adding non-protein silicone oil particles to the preparation of rFVIII. While the size distribution of sub-visible particles was similar for both technologies, the flow-cytometry-based technology appeared to be more sensitive, counting higher absolute numbers of sub-visible particles than the micro-flow imaging technology for all size ranges (Fig. 5a and b).

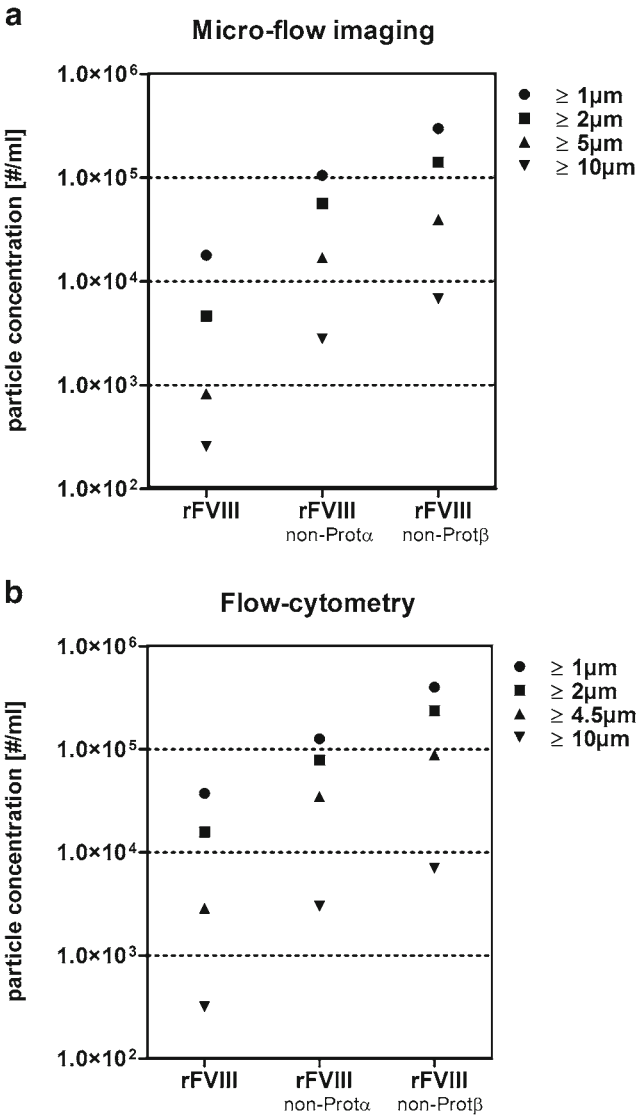

Fig. 5 Comparison of flow-cytometry and micro-flow imaging for the analysis of sub-visible particles. A preparation of rFVIII was mixed with two different non-protein silicone particle preparations (rFVIII+ non-Protα; rFVIII+ non-Protβ) as described in the section Materials and Methods and subsequently analyzed for the concentration of total sub-visible particles in different size ranges. For this purpose, the size ranges of the flow-cytometry-based technology were adapted to the size ranges covered by the micro-flow imaging technology, namely ≥1, ≥2, ≥5 and ≥10 μm. rFVIII without non-protein silicone particles was included as a control. Presented are the means of 3 replicates. The results obtained with the micro-flow imaging technology (**a**) were in good agreement with those obtained with the flow-cytometry-based technology (**b**). Both technologies showed a concentration-dependent increase in sub-visible particle count after adding non-protein silicone oil particles to the preparation of rFVIII.

Interaction Studies of Proteins with Silicone Oil Droplets

Silicone oil is one of the most abundant sources of non-protein sub-visible particles present in protein therapeutics (42). Therefore, we were interested to know if the flow-cytometry-based technology could be used to study interactions of proteins with silicone oil droplets. We used rFVIII as a protein source and D-PBS buffer enriched with silicone oil sub-visible particles. The rFVIII solution, which was filtered through 0.22 µm pores, contained only very few sub-visible particles (Fig. 6a). In contrast, the D-PBS sample enriched with silicone oil particles contained a substantial number of sub-visible particles (Fig. 6b). We mixed the rFVIII solution with silicone oil particles, incubated the mixture for 10 min and subsequently analyzed it for sub-visible particles (0.75–10 µm). The results of this analysis as presented in Fig. 6c and d indicate that the incubation of the rFVIII solution with silicone oil particles generated an increased number of protein-containing particles, as demonstrated by binding to Bis-ANS. At the same time, the number of non-protein particles which did not bind to Bis-ANS was substantially reduced, indicating that silicone oil particles were covered with rFVIII and appeared as protein-containing particles. Figure 6d shows an overlay of Fig. 6b and c for better comparison.

Our results demonstrate that the FACS technology can detect sub-visible particles with a non-protein core (e.g. silicone oil) and a protein surface without the need for prior labeling of either the protein or the silicon oil droplets.

DISCUSSION

Recently, sub-visible particles present in protein therapeutics have received increasing attention because of their potential contribution to the unwanted immunogenicity of protein therapeutics (16). Although a couple of mechanisms have been proposed, the root cause for the induction of unwanted immune responses by sub-visible particles is not completely understood. The design of scientifically sound studies has been complicated by the limited availability of technologies suitable to quantify and characterize the wide variety of sub-visible particles which can be present in protein solutions. Here, we present a flow-cytometry-based technology which uses a combination of forward and side scattering together with fluorescence staining of specific particle features to determine the number, size distribution and specific characteristics of sub-visible particles between 0.75 and 10 µm in size. Flow

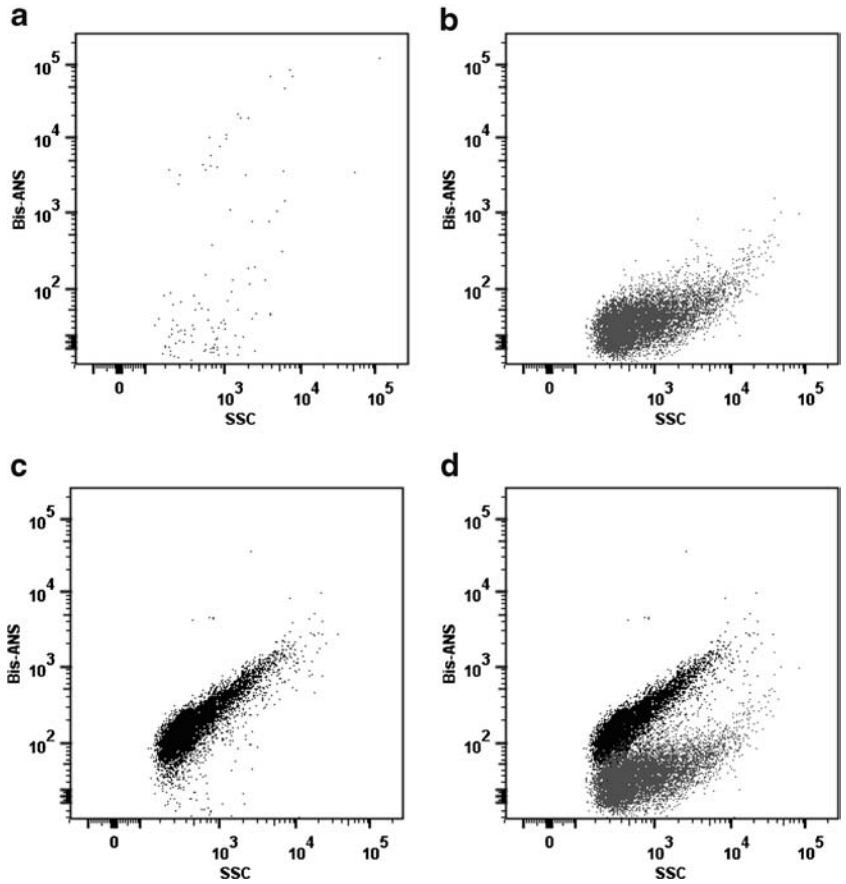

Fig. 6 Detection of particles with a non-protein core and a protein surface. Preparations of rFVIII (**a**), silicone oil particles (**b**) and mixtures of rFVIII and silicone oil particles (**c**) were stained with Bis-ANS and subsequently analyzed for sub-visible particles by the flow-cytometry-based technology as described in the section Materials and Methods. For comparison of the Bis-ANS fluorescence intensities of silicone oil particles (**b**) and the mixture of rFVIII with silicone oil particles (**c**), an overlay of both graphs is presented in (**d**). Whereas the 0.22 μm filtered rFVIII preparation presented in (**a**) contained few sub-visible particles, the preparation of silicone oil particles presented in (**b**) contained a substantial number of sub-visible particles which did not bind Bis-ANS. The mixture of rFVIII with silicone oil particles generated sub-visible particles which bound to Bis-ANS (**c**, **d**). At the same time, particles which did not bind to Bis-ANS disappeared almost completely indicating the generation of particles with a non-protein core and a protein surface (**c**, **d**).

cytometry has only recently been introduced as a potential technology platform for the analysis of sub-visible particles present in solutions of therapeutic proteins (32, 33). Mach *et al.* used SYPRO Orange dye, which binds to hydrophobic surfaces of partially destabilized proteins, to preferentially stain protein-containing particles and measure their numbers in therapeutic preparations of monoclonal antibodies (32). The authors used a Beckman-Coulter FC-500 flow cytometer equipped with a 488-nm argon laser and combined the detection of SYPRO Orange fluorescence with forward and side scattering. Thus, they were able to detect protein particles with a size of ≥1 μm. Ludwig *et al.* applied flow cytometry for the detection and characterization of sub-visible particles in silicone-oil-contaminated protein formulations (33). They used a BD FACS Calibur equipped with two lasers (488 and 635 nm) and combined the detection of two fluorescence dyes (AlexaFluor 647 and BODIPY 493/503) with forward and side scattering. Using proteins pre-labeled with Alexa Fluor 647 and silicone oil pre-stained with BODIPY 493/503, the authors demonstrated that flow cytometry has the ability to discriminate between homogenous protein aggregates and heterogeneous particles made up of silicone oil and protein. They estimated that they were able to analyze sub-visible particles with a size ≥1.8 μm. Nishi *et al.* described the use of flow cytometry for the label-free detection of sub-visible aggregates in liquid IgG1 antibody formulations prepared under different stress conditions (43). The authors used a BD FACS Canto II flow cytometer equipped with two lasers (488 and 633 nm), quantified the particle counts by acquiring all samples for a fixed time and compared their counts with results obtained with MFI and with light obscuration. The authors concluded that all three applied methods provided similar results for total particle counts.

We further explored the suitability of flow cytometry for the analysis of sub-visible particles by using this technology for the simultaneous detection, quantification, size estimation and characterization of sub-visible particles. For this purpose, we optimized the settings of a 3-laser 8-color FACS Canto II flow

cytometer by tuning the forward scatter and the side scatter detectors and by using size calibration beads to facilitate the analysis of sub-visible particles with sizes below 1 μm. This way, we could reproducibly detect and characterize particles as small as 0.75 μm. This lower limit of detection for the particle size might be further reduced to 0.1 μm by using specialized flow cytometers with improved optics and an optimized detector design (44). Importantly, the particle size is always an estimate because the refractive index of the particle, which influences the size determination by flow cytometry (45), is different for each particle and therefore unknown. Moreover, the morphology of the particle influences size determination. In contrast to amorphous particles, the detected size for a particle with a needle-like structure depends on the angle of the particle when it passes the interrogation point of the flow cytometer. Taking both aspects into consideration, it is important to emphasis that the presented flow-cytometry-based technology facilitates comparative analysis of samples containing the same protein. It should not be used to compare samples containing completely different proteins.

We paid particular attention to the capacity of the FACS technology to detect single particles rather than swarms of small particles. Analyzing serial dilutions of particle solutions, we generated data sets which support this capacity. However, we are aware that protein aggregates are in a thermodynamic equilibrium (46). They can change their morphology or return to their monomeric structure upon dilution. The linear decrease of particle count and size distribution, in correlation with the samples dilutions, demonstrated that the protein aggregates remained intact and did not separate into their building blocks when diluted under our experimental set ups. It is accepted, that protein aggregates, especially those containing cross-β-sheet structures, are at local energetic minimum, which facilitates the use of analytical tools for *in vitro* analysis of these aggregates (46). To further minimize any potential destabilizing effect of the analytical procedure on the stability of protein aggregates, the analysis should preferentially be done in the final protein formulation. The presented FACS technology is well suited to analyze samples in the final protein formulation. Flow cytometry data related to the size distribution of particles in protein solutions were in good agreement with data generated with the state-of-the art technology micro-flow imaging. However, the flow-cytometry-based technology seemed to be more sensitive which was reflected by counting higher absolute numbers of particles for each size range. We believe that the use of fluorescent dyes may circumvent detection problems that are related to translucent proteins (47, 48) which could be the reason for the higher sensitivity of the flow-cytometry-based technology.

A major advantage of flow-cytometry-based technologies for the analysis of sub-visible particles is the possibility to combine forward and side scattering with fluorescence detection. The BD FACS Canto II we used for our analysis is equipped with 3 lasers (405, 488, and 630 nm) and offers the maximum capacity of analyzing 8 different fluorescence colors on one particle. This setting would allow a comprehensive assessment of the major characteristics of each sub-visible particle provided that suitable fluorescence dyes which bind to specific structures of protein and non-protein particles become available.

When we initiated this study our major objective was to combine a fluorescence dye which binds to proteins and another dye which binds to cross-ß-sheet structures contained in proteins. We tested several different combinations of dyes and eventually chose Bis-ANS as a protein stain and DCVJ as a stain for cross-β-sheet structures in proteins. Given our optimized instrument settings for the BD FACS Canto II, the combination of these two dyes showed the best performance with respect to signal to noise ratio, reproducibility of staining and minimal cross-talk of the dyes into other filters. Nevertheless, we could not completely prevent some limited cross-talk between the two dyes. DCVJ fluorescence, the stain for cross-β-sheet structures shows some cross-talk into the channel for protein detection by Bis-ANS fluorescence. However, this cross-talk should not generate any analytical problem because all cross-β-sheet positive particles are protein particles.

Although we were able to differentiate all proteins included in our study from non-protein particles, we are aware that the binding of fluorescent dyes is influenced by the nature of the protein and the nature of the protein aggregate. Therefore, we would like to re-emphasize that the flow-cytometry-based technology facilitates comparative analysis of samples containing the same protein. It should not be used to compare samples containing completely different proteins.

Using the flow-cytometry-based technology presented in this manuscript, we could clearly distinguish between non-protein particles such as silicone oil droplets and protein particles and could also study the interaction of proteins with silicone droplets. For method development, we used artificially high concentrations of silicone oil droplets. However, we do not consider these high concentrations to affect interactions between proteins and silicone oil droplets. Silicone oil presents one of the major sources for non-protein particles in formulations of protein therapeutics, especially if the proteins are formulated in prefilled glass syringes. These syringes are usually lubricated with silicone oil, which is sprayed onto the interior surfaces of the syringe during the syringe manufacturing process, to allow for smooth plunger movement (49). Our data indicate that proteins can attach to the surface of silicone oil droplets creating particles with a non-protein core and a protein surface. These data confirm previous findings by Ludwig *et al.* (33). Characterization of additional properties of proteins coated on silicone oil droplets (e.g. presence of cross-ß-sheet structure or of other structural characteristics) may provide important additional information in the future.

In summary, we established a flow-cytometry-based technology for the analysis of sub-visible particles in protein

formulations that facilitates the simultaneous analysis of size distribution, number and specific features of particles with a size range of 0.75–10 μm. The benefits of this technology are the relatively short time required for the analysis of each sample and the relatively small amount of required sample volume.

ACKNOWLEDGMENTS AND DISCLOSURES

The authors thank Elise Langdon-Neuner and Karima Benamara for editing the manuscript.

This work was supported by Baxter Innovation GmbH. C.L., M.M., T.P., T.W., P.M., P.L.T., F.S. and B.M.R. are employees of Baxter Innovation GmbH.

Authors Contribution C. L. designed research, performed flow cytometric analysis, analyzed and interpreted data, and wrote the paper; M.M. designed research, analyzed and interpreted data, and wrote the paper; T.P. performed flow cytometric analysis, and analyzed and interpreted data, T.W. performed flow cytometric analysis of the method validation; P.M. performed, analyzed and interpreted micro flow imaging data; P.L.T. interpreted data; F.S. interpreted data; B.M.R. designed research, analyzed and interpreted data, and wrote the paper.

REFERENCES

1. Leader B, Baca QJ, Golan DE. Protein therapeutics: a summary and pharmacological classification. Nat Rev Drug Discov. 2008;7(1):21–39.
2. Büttel IC, Chamberlain P, Chowers Y, Ehmann F, Greinacher A, Jefferis R, et al. Taking immunogenicity assessment of therapeutic proteins to the next level. Biologicals. 2011;39(2):100–9.
3. Baker MP, Reynolds HM, Lumicisi B, Bryson CJ. Immunogenicity of protein therapeutics: the key causes, consequences and challenges. Self Nonself. 2010;1(4):314–22.
4. Schellekens H. The immunogenicity of therapeutic proteins. Discov Med. 2010;9:560–4.
5. Casadevall N, Nataf J, Viron B. Pure red-cell aplasia and anti-erythropoietin antibodies in patients treated with recombinant erythropoietin. N Engl J Med. 2002;346:469–75.
6. Everds NE, Tarrant JM. Unexpected hematologic effects of biotherapeutics in nonclinical species and in humans. Toxicol Pathol. 2013;41:280–302.
7. Farrell RA, Marta M, Gaeguta AJ. Development of resistance to biologic therapies with reference to IFNb. Rheumatology. 2012;51:590–9.
8. Ratanji KD, Derrick JP, Dearman RJ, Kimber IJ. Immunogenicity of therapeutic proteins: influence of aggregation. J Immunotoxicol. 2014;11(2):99–109.
9. Rosenberg AS. Effects of protein aggregates: an immunologic perspective. AAPS J. 2006;8:501–7.
10. Sauerborn M, Brinks V, Jiskoot W, Schellekens H. Immunological mechanism underlying the immune response to recombinant human protein therapeutics. Trends Pharmacol Sci. 2010;31:53–9.
11. Aguzzi A, O'Connor T. Protein aggregation diseases: pathogenicity and therapeutic perspectives. Nat Rev Drug Discov. 2010;9(3):237–48.
12. Sawaya MR, Sambashivan S, Nelson R, Ivanova MI, Sievers SA, Apostol MI, et al. Atomic structures of amyloid cross-beta spines reveal varied steric zippers. Nature. 2007;447(7143):453–7.
13. Maas C, Hermeling S, Bouma B, Jiskoot W, Gebbink MF. A role for protein misfolding in immunogenicity of biopharmaceuticals. J Biol Chem. 2007;282(4):2229–36.
14. Gustot A, Raussens V, Dehousse M, Dumoulin M, Bryant CE, Ruysschaert JM, et al. Activation of innate immunity by lysozyme fibrils is critically dependent on cross-β sheet structure. Cell Mol Life Sci. 2013;70(16):2999–3012.
15. Salminen A, Ojala J, Kauppinen A, Kaarniranta K, Suuronen T. Inflammation in Alzheimer's disease: amyloid-beta oligomers trigger innate immunity defence via pattern recognition receptors. Prog Neurobiol. 2009;87(3):181–94.
16. Wang W, Singh SK, Li N, Toler MR, King KR, Nema S. Immunogenicity of protein aggregates–concerns and realities. Int J Pharm. 2012;431(1–2):1–11.
17. Engelsman J, Garidel P, Smulders R, Koll H, Smith B, Bassarab S, et al. Strategies for the assessment of protein aggregates in pharmaceutical biotech product development. Pharm Res. 2011;28:920–33.
18. Wiesbauer J, Prassl R, Nidetzky B. Renewal of the air-water interface as a critical system parameter of protein stability: aggregation of the human growth hormone and its prevention by surface-active compounds. Langmuir. 2013;29(49):15240–50.
19. Wang W. Lyophilization and development of solid protein pharmaceuticals. Int J Pharm. 2000;203(1–2):1–60.
20. Stathopulos PB, Scholz GA, Hwang YM, Rumfeldt JA, Lepock JR, Meiering EM. Sonication of proteins causes formation of aggregates that resemble amyloid. Protein Sci. 2004;13(11):3017–27.
21. Ruiz L, Reyes N, Aroche K, Tolosa V, Simanca V, Rogríguez T, et al. Influence of packaging material on the liquid stability of interferon-alpha2b. J Pharm Sci. 2005;8(2):207–16.
22. Gerhardt A, Mcgraw NR, Schwartz DK, Bee JS, Carpenter JF, Randolph TW. Protein aggregation and particle formation in prefilled glass syringes. J Pharm Sci. 2014;103(6):1601–12.
23. Chi EY, Weickmann J, Carpenter JF, Manning MC, Randolph TW. Heterogeneous nucleation-controlled particulate formation of recombinant human platelet-activating factor acetylhydrolase in pharmaceutical formulation. J Pharm Sci. 2005;94(2):256–74.
24. Akers MJ, Vasudevan V, Stickelmyer M. Formulation development of protein dosage forms. In: Nail SL, Akers MJ, editors. Development and manufacture of protein pharmaceuticals. New York: Kluwer Academic/Plenum Press; 2002. p. 47–127.
25. Tyagli AK, Randolph TW, Dong A, Maloney KM, Hitscherich Jr C, Carpenter JF. IgG particle formation during filling pump operation: a case study of heterogeneous nucleation on stainless steel nanoparticles. J Pharm Sci. 2009;98:94–104.
26. Kerwin BA, Akers MJ, Apostol I, Moore-Einsel C, Etter JE, Hess E, et al. Acute and long-term stability studies of deoxy hemoglobin and characterization of ascorbate-induced modifications. J Pharm Sci. 1999;88:79–88.
27. Hawe A, Friess W. Stabilization of a hydrophobic recombinant cytokine by human serum albumin. J Pharm Sci. 2007;96:2987–99.
28. Jones LS, Kaufmann A, Middaugh CR. Silicone oil induced aggregation of proteins. J Pharm Sci. 2005;94:918–27.
29. Thirumangalathu R, Krishnan S, Ricci MS, Brems DN, Randolph TW, Carpenter JF. Silicone oil- and agitation-induced aggregation of a monoclonal antibody in aqueous solution. J Pharm Sci. 2009;98:3167–81.
30. Carpenter JF, Randolph TW, Jiskoot W. Overlooking subvisible particles in therapeutic protein products: gaps that may compromise product quality. J Pharm Sci. 2009;98:1201–5.

31. Palutke M, KuKuruga D, Wolfe D, Roher A. Flow cytometric purification of Alzheimer's disease amyloid plaque core protein using thioflavin T. Cytometry. 1987;8(5):494–9.
32. Mach H, Bhambhani A, Meyer BK, Burek S, Davis H, Blue JT, et al. The use of flow cytometry for the detection of subvisible particles in therapeutic protein formulations. J Pharm Sci. 2011;100(5):1671–8.
33. Ludwig DB, Trotter JT, Gabrielson JP, Carpenter JF, Randolph TW. Flow cytometry: a promising technique for the study of silicone oil-induced particulate formation in protein formulations. Anal Biochem. 2011;410(2):191–9.
34. Ostman J, Darinskas A, Zamotin V, Liutkevicius E, Lundgren E, Morozova-Roche LA. Does the cytotoxic effect of transient amyloid oligomers from common equine lysozyme in vitro imply innate amyloid toxicity? J Biol Chem. 2005;280(8):6269–75.
35. Lindgren M, Sörgjerd K, Hammarström P. Detection and characterization of aggregates, prefibrillar amyloidogenic oligomers, and protofibrils using fluorescence spectroscopy. Biophys J. 2005;88(6): 4200–12.
36. Bertoncini CW, Celej MS. Small molecule fluorescent probes for the detection of amyloid self-assembly in vitro and in vivo. Curr Protein Pept Sci. 2011;12(3):205–20.
37. Paslawski W, Andreasen M, Nielsen SB, Lorenzen N, Thomsen K, Kaspersen JD, et al. High stability and cooperative unfolding of α-synuclein oligomers. Biochemistry. 2014;53(39):6252–63.
38. EMA, Committee for Medicinal Products for Human Use. EMEA/CHMP/EWP/192217/2009 Guideline on Bioanalytical Method Validation. February 2012.
39. US Department of Health and Human Services, Food and Drug Administration, Center for Drug Evaluation and Research (CDER) and Center for Biologics Evaluation and Research (CBER). Draft guidance for industry: assay development for immunogenicity testing of therapeutic proteins. December 2009.
40. Nolan JP, Stoner SA. A trigger channel threshold artifact in nanoparticle analysis. Cytometry A. 2013;83:301–5.
41. van der Vlist EJ, Nolte-'t Hoen EN, Stoorvogel W, Arkesteijn GJ, Wauben MH. Fluorescent labeling of nano-sized vesicles released by cells and subsequent quantitative and qualitative analysis by high-resolution flow cytometry. Nat Protoc. 2012;7:1311–26.
42. Wen ZQ, Torraca G, Yee CY, Li G. Investigation of contaminants in protein pharmaceuticals in pre-filled syringes by multiple micro-spectroscopies. Am Pharm Rev. 2007;10:101–7.
43. Nishi H, Mathäs R, Fürst R, Winter G. Label-free flow cytometry analysis of subvisible aggregates in liquid IgG1 antibody formulations. J Pharm Sci. 2014;103(1):90–9.
44. van der Pol E, Coumans FA, Grootemaat AE, Gardiner C, Sargent IL, Harrison P, et al. Particle size distribution of exosomes and microvesicles determined by transmission electron microscopy, flow cytometry, nanoparticle tracking analysis, and resistive pulse sensing. J Thromb Haemost. 2014;12(7):1182–92.
45. Shapiro HM. Practical flow cytometry, 4th edition. Vienna, Austria: Wiley-Liss; 2003.
46. Jahn TR, Radford SE. The Yin and Yang of protein folding. FEBS J. 2005;272(23):5962–70.
47. Wuchner K, Büchler J, Spycher R, Dalmonte P, Volkin DB. Development of a microflow digital imaging assay to characterize protein particulates during storage of a high concentration IgG1 monoclonal antibody formulation. J Pharm Sci. 2010;99:3343–61.
48. Zölls S, Gregoritza M, Tantipophan R, Wiggenhorn M, Winter G, Friess W, et al. How subvisible particles become invisible—relevance of the refractive index for protein particle analyses. J Pharm Sci. 2013;102:1434–46.
49. Fries A. Drug delivery of sensitive biopharmaceuticals with prefilled syringes. Drug Deliv Technol. 2009;9:22–7.